Remote Sensing Image Fusion

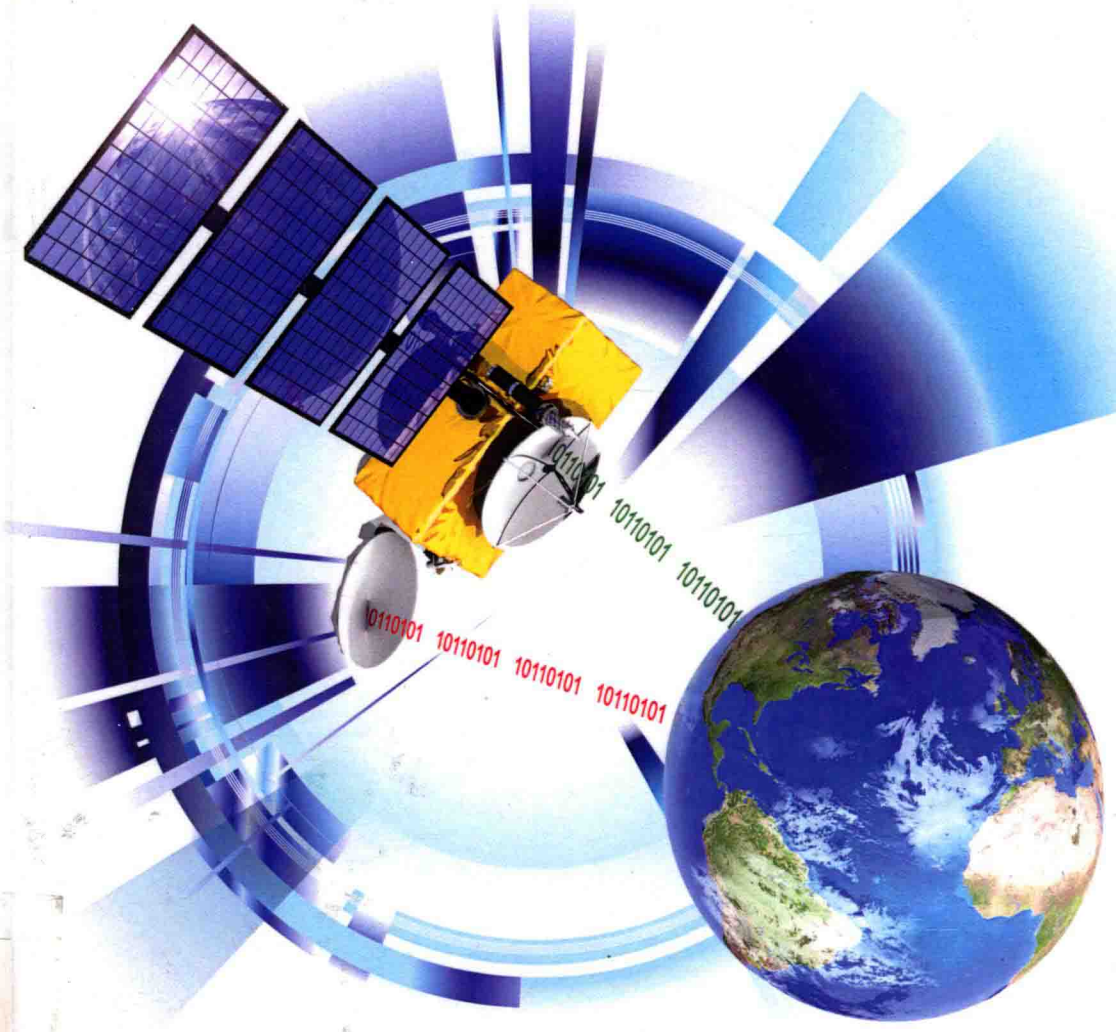

Luciano Alparone • Bruno Aiazzi
Stefano Baronti • Andrea Garzelli

CRC Press
Taylor & Francis Group

Remote Sensing Image Fusion

Luciano Alparone • Bruno Aiazzi
Stefano Baronti • Andrea Garzelli

CRC Press
Taylor & Francis Group
Boca Raton London New York

CRC Press is an imprint of the
Taylor & Francis Group, an **informa** business

CRC Press
Taylor & Francis Group
6000 Broken Sound Parkway NW, Suite 300
Boca Raton, FL 33487-2742

Printed on acid-free paper
Version Date: 20150113

International Standard Book Number-13: 978-1-4665-8749-6 (Hardback)

Visit the Taylor & Francis Web site at
http://www.taylorandfrancis.com

and the CRC Press Web site at
http://www.crcpress.com

Remote Sensing Image Fusion

Signal and Image Processing of Earth Observations Series

Series Editor

C.H. Chen

Published Titles

Remote Sensing Image Fusion
Luciano Alparone, Bruno Aiazzi, Stefano Baronti, and Andrea Garzelli

Preface

Nowadays, approximately four TB of image data are collected daily by instruments mounted on satellite platforms, not to mention the data produced by a myriad of specific campaigns carried out through airborne instruments. Very high-resolution (VHR) multispectral scanners, IKONOS, QuickBird, GeoEye, WorldView, Pléiades, just to mention the most popular, and especially the related monospectral panchromatic instruments are responsible for a large part of the amount. Imaging spectrometers with tens to hundreds of bands will significantly contribute after the launch of the upcoming PRISMA and EnMap missions. In parallel, synthetic aperture radar (SAR) satellite constellation systems, TerraSAR-X/Tandem-X, COSMO-SkyMed, RadarSat-2, and the upcoming RadarSat-3 and Sentinel-2 are taking high-resolution microwave images of the Earth with ever improved temporal repetition capabilities.

The availability of image data with spectral diversity (visible, near infrared, short wave infrared, thermal infrared, X- and C-band microwaves with related polarizations) and complementary spectral-spatial resolution, together with the peculiar characteristics of each image set, have fostered the development of fusion techniques specifically tailored to remotely sensed images of the Earth. Fusion aims at producing an extra value with respect to those separately available from the individual datasets. Though the results of fusion are more often analyzed by human experts to solve specific tasks (detection of landslides, flooded and burned areas, just to mention a few examples), partially supervised and also fully automated systems, most notably thematic classifiers, have started benefiting from fused images instead of separate datasets.

The most prominent fusion methodology specifically designed for remote sensing images is the so-called panchromatic sharpening or *pansharpening*, which in general requires the presence of a broadband in the visible or visible near-infrared (V-NIR) wavelengths, with ground resolution that is two to six times greater than that of the narrow spectral bands. Multispectral pansharpening can be brought back to the launch of the first SPOT instrument, which was first equipped with a panchromatic scanner together with the multispectral one. Recently, hyperspectral pansharpening has also started being investigated by an increasing number of scientists, with the goal, for example, of coupling spatial and spectral detection capabilities in a unique image.

The fusion of images from heterogeneous datasets, that is, of images produced by independent modalities that do not share either wavelengths or imaging mechanisms is a further task, which is pursued in remote sensing ap-

plications. A notable example is the sharpening of thermal bands through simultaneous visible near-infrared observations. This issue has also been largely addressed outside the scope of remote sensing, for detection applications, both military and civilian.

A more unconventional and specific topic is the fusion of optical and SAR image data. Several fusion methods, in which an optical image is enhanced by a SAR image, have been developed for specific applications. The all-weather acquisition capability of SAR systems, however, makes a product with opposite features to appear even more attractive. The availability of a SAR image spectrally and/or spatially enhanced by an optical observation with possible spectral diversity is invaluable, especially because the optical data may not always be available, particularly in the presence of cloud covers, while SAR platforms capture images regardless of sunlight and meteorological conditions.

Symbol Description

$\boldsymbol{\alpha}$	Sparse vector in compressed sensing pansharpening.
$\tilde{\mathbf{A}}_k$	Interpolated aliasing pattern of the kth MS band.
$\tilde{\mathbf{A}}_P$	Interpolated aliasing pattern of Pan.
β	Multiplicative factor for the CSA method.
$\mathbf{B}_k$	Original kth image band.
$\tilde{\mathbf{B}}_k$	kth image band interpolated to Pan scale.
$\hat{B}_k$	Pansharpened kth image band.
δ	Spatial detail image.
$\delta(\Delta x, \Delta y)$	Spatial detail image in the presence of Pan-MS misalignment.
$\boldsymbol{D}$	Dictionary matrix in compressed sensing pansharpening.
D_λ	Spectral distortion.
D_s	Spatial distortion.
Δx	Horizontal spatial misalignment between Pan and interpolated MS.
Δy	Vertical spatial misalignment between Pan and interpolated MS.
$\mathbf{D}_x^{(I)}$	Derivative of $\mathbf{I}$ in the x direction.
$\mathbf{D}_y^{(I)}$	Derivative of $\mathbf{I}$ in the y direction.
$\mathbf{D}_x^{(k)}$	Derivative of $\tilde{\mathbf{M}}_k$ in the x direction.
$\mathbf{D}_y^{(k)}$	Derivative of $\tilde{\mathbf{M}}_k$ in the y direction.
$\mathbf{F}$	Sparse matrix in restoration-based pansharpening.
$\mathbf{g}^*$	Highpass filter impulse response for GLP schemes.
g_k	Global injection gain of the kth band.
$\mathbf{G}_k$	Space-varying local injection gain of the kth band.
h_j^*	Equivalent lowpass impulse response of the jth level of ATW.
H_j^*	Equivalent lowpass frequency response of the jth level of ATW.
H_k	PSF for the kth band in restoration-based pansharpening.
$\mathbf{I}$	Intensity image.
$\mathbf{I}(\Delta x, \Delta y)$	Intensity image in the presence of Pan-MS misalignment.
$\mathbf{I}_k$	Intensity image for the kth band in the BDSD method.
K	Number of bands.
$\tilde{\mathbf{M}}_k$	Original kth MS band expanded to the Pan scale.
$\hat{\mathbf{M}}_k$	Pansharpened kth MS band.
$\hat{\mathbf{M}}_k(\Delta x, \Delta y)$	Pansharpened kth MS band in the presence of Pan-MS misalignment.
$\tilde{\mathbf{M}}_k^*$	Interpolated aliasing free kth MS band.
$\hat{\mathbf{M}}_k^*$	Pansharpened kth band obtained from aliasing free Pan and MS.
p	Integer reduction factor for GLP.
$\mathbf{P}$	Panchromatic image.

q	Integer expansion factor for GLP.
Q	Universal Image Quality Index.
$Q2^n$	Generalization of $Q4$ to 2^n-band images.
$Q4$	Extension of the Universal Image Quality Index to 4-band images.
$\mathbf{P}_L$	Lowpass-filtered panchromatic image.
$\mathbf{P}_L^*$	Lowpass-filtered Pan downsampled by r and then interpolated by r.
r	Spatial sampling ratio between original MS and Pan.
θ	Soft threshold of modulating SAR texture.
$\mathbf{t}$	Texture image extracted from SAR for optical-SAR fusion.
$\mathbf{t}_\theta$	Texture image $\mathbf{t}$ thresholded by θ.
$\mathbf{T}_k$	kth TIR band.
$\widetilde{\mathbf{T}}_k$	kth TIR band interpolated to the scale of the V-NIR band.
$\widehat{\mathbf{T}}_k$	Spatially enhanced kth TIR band.
$\mathbf{V}$	Enhancing V-NIR band.
$\mathbf{V}_L$	Lowpass-filtered version of $\mathbf{V}$.
$\mathbf{V}_L^*$	Lowpass-filtered $\mathbf{V}$ downsampled by r and then interpolated by r.
w_k	Spectral weight of the kth band for intensity computation.
$w_{k,l}$	Spectral weight of the lth band for $\mathbf{I}_k$ computation.

List of Acronyms

ADC	Analog-to-Digital Converter
ALI	Advanced Land Imager
ASI	Agenzia Spaziale Italiana
ASC-CSA	Agence Spatiale Canadienne-Canadian Space Agency
ATW	À Trous Wavelet
AVHRR	Advanced Very High Resolution Radiometer
BDSD	Band Dependent Spatial Detail
CC	Correlation Coefficient
CCD	Charge-Coupled Device
CNES	Centre Nationale d'Etudes Spatiales
CST	Compressed Sensing Theory
COSMO	COnstellation of small Satellites for Mediterranean basin Observation
CS	Component Substitution
CSA	Constrained Spectral Angle
DEM	Digital Elevation Model
DFB	Directional Filter Bank
DLR	Deutsches zentrum für Luft- und Raumfahrt
DTC	Dual-Tree Complex
DWT	Discrete Wavelet Transform
EHR	Extremely High Resolution
ELP	Enhanced Laplacian Pyramid
ELR	Extremely Low Resolution
EMR	ElectroMagnetic Radiation
EnMAP	Environmental Monitoring and Analysis Program
ENVI	ENvironment for Visualizing Images
EnviSat	Environmental Satellite
ERGAS	Erreur Relative Globale Adimensionnelle de Synthèse
ERS	European Remote-Sensing satellite
ESA	European Space Agency
FOV	Field Of View
GGP	Generalized Gaussian Pyramid
GIHS	Generalized Intensity-Hue-Saturation
GLP	Generalized Laplacian Pyramid
GP	Gaussian Pyramid
GPS	Global Positioning System
GS	Gram-Schmidt

HPF	High Pass Filtering
HPM	High Pass Modulation
HS	HyperSpectral
IFOV	Instantaneous Field Of View
IHS	Intensity-Hue-Saturation
IMU	Inertial Measurement Unit
JERS	Japanese Earth Resources Satellite
JPL	Jet Propulsion Laboratory
KoMPSat	Korean Multi Purpose Satellite
LASER	Light Amplification by Stimulated Emission of Radiation
LiDAR	Light Detection And Ranging
LP	Laplacian Pyramid
LWIR	Long Wave InfraRed
MeR	Medium Resolution
MMSE	Minimum Mean Square Error
MoR	Moderate Resolution
MRA	MultiResolution Analysis
MS	MultiSpectral
MSE	Mean Square Error
MTF	Modulation Transfer Function
MWIR	Medium Wave InfraRed
NASA	National Aeronautics and Space Administration
NDVI	Normalized Differential Vegetation Index
NIR	Near InfraRed
NN	Nearest Neighbor
NSCT	NonSubsampled Contourlet Transform
NSDFB	NonSubsampled Directional Filter Bank
NSP	NonSubsampled Pyramid
OLI	Operational Land Imager
OTF	Optical Transfer Function
PCA	Principal Component Analysis
PR	Perfect Reconstruction
PRF	Pulse Repetition Frequency
PRISMA	PRecursore IperSpettrale della Missione Applicativa
PSF	Point Spread Function
QFB	Quincunx Filter Bank
QMF	Quadrature Mirror Filter
QNR	Quality with No Reference
RCM	RadarSat Constellation Mission
RMSE	Root Mean Square Error
RS	Remote Sensing
SAM	Spectral Angle Mapper
SAR	Synthetic Aperture Radar
SHALOM	Spaceborne Hyperspectral Applicative Land and Ocean Mission
SIR	Shuttle Imaging Radar

SLAR	Side-Looking Airborne Radar
SNR	Signal-to-Noise Ratio
SPOT	Satellite Pour l'Observation de la Terre
SRTM	Shuttle Radar Topography Mission
SS	SuperSpectral
SSI	Spatial Sampling Interval
SWIR	Short Wave InfraRed
SWT	Stationary Wavelet Transform
TDI	Time Delay Integration
TIR	Thermal InfraRed
UDWT	Undecimated Discrete Wavelet Transform
UIQI	Universal Image Quality Index
UNBPS	University of New Brunswick PanSharp
US	UltraSpectral
VIR	Visible InfraRed
VIRS	Visible and InfraRed Scanner
VHR	Very High Resolution
V-NIR	Visible Near-InfraRed
WPD	Wavelet Packet Decomposition

Contents